



The evolution of low-mass, close binary systems with a neutron star component: a detailed grid

M. A. De Vito^{1,2}† and O. G. Benvenuto^{1,2}‡

¹Facultad de Ciencias Astronómicas y Geofísicas, Universidad Nacional de La Plata (UNLP), Paseo del Bosque S/N, B1900FWA La Plata, Argentina

²Instituto de Astrofísica de La Plata, IALP, CCT-CONICET-UNLP, B1900FWA La Plata, Argentina

Accepted 2011 December 27. Received 2011 December 27; in original form 2010 September 17

ABSTRACT

In close binary systems composed of a normal donor star and an accreting neutron star, the amount of material received by the accreting component is, so far, a real intrigue. In the literature, there are available models that link the accretion disc surrounding the neutron star with the amount of material it receives, but there is no model linking the amount of matter lost by the donor star to that falling on to the neutron star.

In this paper, we explore the evolutionary response of these close binary systems when we vary the amount of material accreted by the neutron star. We consider a parameter β which represents the fraction of material lost by the normal star that can be accreted by the neutron star. β is considered as constant throughout the evolution. We have computed the evolution of a set of models considering initial donor star masses M_i/M_\odot between 0.5 and 3.50, initial orbital periods P_i/d between 0.175 and 12, initial masses of neutron stars $(M_{NS})_i/M_\odot$ of 0.80, 1.00, 1.20 and 1.40 and several values of β . We assumed solar abundances. These systems evolve to ultracompact or to open binary systems, many of which form low-mass helium white dwarfs. We present a grid of calculations and analyse how these results are affected upon changes in the value of β . We find a weak dependence of the final donor star mass on β . In most cases, this is also true for the final orbital period. The most sensitive quantity is the final mass of the accreting neutron star.

As we do not know the initial mass and rotation rate of the neutron star of any system, we find that performing evolutionary studies is not helpful for determining β .

Key words: binaries: close – stars: evolution – white dwarfs.

1 INTRODUCTION

It is currently accepted that close binary systems (CBSs) composed of a white dwarf (WD) and a millisecond pulsar (MSP) are the result of the evolution of a normal main-sequence donor star together with a rotating neutron star (NS). These systems, also, are considered to give rise to the occurrence of low-mass X-ray binary (LMXB) sources (see e.g. Podsiadlowski, Rappaport & Pfahl 2002).

The standard model states that when a normal star fills its Roche lobe, it starts to transfer mass to its NS companion. The material forms an accretion disc around the compact star, and a part of the transferred mass is deposited on to the NS surface. The NS rotation is

accelerated due to angular momentum deposition on its surface, thus becoming an MSP (for a review, see Bhattacharya & van den Heuvel 1991). In order to compute the evolution of CBSs, we have to make some hypotheses on the characteristics of mass transfer. Usually, this problem has been handled considering a two-parameter description. These are the fraction of mass lost by the donor star that can be accreted by its companion (β) and the amount of specific angular momentum carried out from the system (α). Both quantities are assumed as constants during the entire stellar evolution. The value of β has been usually set to $\beta = 0.5$ (Podsiadlowski, Joss & Hsu 1992; Tauris & Savonije 1999; Podsiadlowski et al. 2002; Nelson & Rappaport 2003). In some cases, it has been set to $\beta = 1$ ($\beta = 0$), which represents a fully conservative (non-conservative) situation (Ergma, Sarna & Antipova 1998). Other values of β have been considered to fit a particular binary system (Benvenuto, Rohrmann & De Vito 2006). Meanwhile, it has been usual to set $\alpha = 1$.

The knowledge of β is, in principle, important for the binary evolution models. Its value directly determines the rate of change of the NS mass, which affects the mass ratio, and then the radius of the Roche lobe R_L (Eggleton 1983). β enters in the differential equation

*E-mail: adevito@fcaglp.unlp.edu.ar (MADV); obenvenuto@fcaglp.unlp.edu.ar (OGB)

†Member of the Carrera del Investigador Científico, Consejo Nacional de Investigaciones Científicas y Técnicas (CONICET).

‡Member of the Carrera del Investigador Científico, Comisión de Investigaciones Científicas de la Provincia de Buenos Aires (CIC).

that determines the evolution of the orbital semi-axis which, in turn, determines the size of the Roche lobe. Thus, β affects the occurrence of Roche lobe episodes. However, unfortunately, neither observational evidence nor theoretical models allow us to infer how much of the matter lost by the donor star is accreted by the NS. Besides, there is an upper limit for the accretion rate given by the Eddington accretion rate $\dot{M}_{\text{Edd}} = 2 \times 10^{-8} M_{\odot} \text{ yr}^{-1}$. To date, β has been considered as a free parameter. Now, we may ask a question. Can β be estimated studying the overall evolution of these CBSs, as well as its temporal evolution? To look for the answer is the main aim of this paper.

It is known that the appearance and variability of accreting millisecond X-ray pulsars strongly depend on the accretion rate on to the NS, \dot{M}_{NS} , the effective viscosity and diffusivity of the disc magnetosphere boundary. For a typical NS with a period of rotation of 2.5 ms, Romanova et al. (2008) present the following classification of accreting NSs as a function of \dot{M}_{NS} . At the *boundary layer* regime, if the accretion rate is sufficiently large ($\dot{M}_{\text{NS}} > 7.3 \times 10^{-8} M_{\odot} \text{ yr}^{-1}$), the star's magnetic field is completely buried (screened) by the accreting matter that falls on to the star directly through the boundary layer. As the accretion rates decrease, the role played by the stellar magnetic field becomes more important, so that it influences the flow of matter around the star. When the mass transfer rate is sufficiently low ($1.3 \times 10^{-11} < \dot{M}_{\text{NS}} < 1.4 \times 10^{-9} M_{\odot} \text{ yr}^{-1}$), the magnetosphere radius becomes larger than the corotation radius, and the star enters the *propeller* regime. In the strong propeller regime, disc matter acquires angular momentum from the rotating magnetosphere fast enough that most of it is ejected by a conical outflow. At the same time, a significant amount of angular momentum and energy flow along the open stellar field lines, giving axially symmetric jets. Finally, for even smaller accretion rates ($\dot{M}_{\text{NS}} < 1.3 \times 10^{-11} M_{\odot} \text{ yr}^{-1}$), accretion on to the NS surface is suppressed, and the star becomes a pulsar. This is the *pulsar* regime. Evidently, there is an important relation between the magnetic field intensity of the NS and its accretion rate. The above given values for these regimes should increase for a stronger magnetic field. Thus, to find β we would need to compute the NS magnetic field evolution.

In the standard model of accreting NSs [or black holes (BH)], the system NS (BH)–accretion disk is considered (Shakura & Sunyaev 1973, 1976; White, Stella & Parmar 1988; Mitsuda et al. 1989; Church, Inogamov & Balucińska-Church 2002; Kulkarni & Romanova 2009). The structure and radiation of stationary discs around NSs is determined by several parameters: the mass of the NS, the accretion rate, the level of turbulence and/or small-scale magnetic fields, etc. If matter flows through the inner boundary at a rate substantially higher than \dot{M}_{Edd} , the gas should flow away perpendicularly from the inner region of the disc driven by radiation pressure. Many authors have developed models of two and three components in order to account for the observed emission spectra in these NS (BH)–accretion disc systems. However, these models do not link the amount of matter lost by the donor star that is accreted by the NS (BH).

Takahashi & Makishima (2006) show that the energy spectra of 18 LMXBs are successfully accounted for by a model consisting of a canonical NS ($M_{\text{NS}} = 1.40 M_{\odot}$) with $\dot{M}_{\text{NS}} < \dot{M}_{\text{Edd}}$. They consider a combination of two optically thick components, one due to the accretion disc and the other radiated by the NS surface. As the accretion rate increases, the disc luminosity increases, but the emission from the NS surface saturates or even decreases. When $\dot{M}_{\text{NS}} \gtrsim \dot{M}_{\text{Edd}}$, the LMXB spectrum consists of three optically thick components: the softest from a retreated disc, the hardest from the

NS surface and an intermediate component presumably due to the outflows caused by the increased radiation pressure.

Again, we could establish a link between the type of model that fits the energy spectrum of these objects and \dot{M}_{NS} . Then, according to the best fit to the energy spectrum of the NS, we could model the accretion on to the NS and consequently model β . In any case, the value of β found in this way corresponds to the very short time-scale of observations, while in evolutionary studies we need the value of β averaged on far longer time periods.

Evidently, computing β from first principles is a very difficult task. It may be considered that a way to find β is to compute the effects on the evolution of CBSs induced by changes in β . In order to explore the viability of such strategy, in this paper we compute a grid of evolutionary models. We consider the evolution of solar composition donor star members of CBSs for a wide range of initial parameters [masses for the donor star M_i and accreting NS ($M_{\text{NS}})_i$, and orbital periods P_i]. Also, we consider different values for β (between 0 and 1, with $\Delta\beta = 0.25$) for the cases of $(M_{\text{NS}})_i/M_{\odot} = 0.80, 1.00$ and 1.20 , and with $\Delta\beta = 0.125$ for the case of $(M_{\text{NS}})_i/M_{\odot} = 1.40$ extending our previous calculations (with $\beta = 0.5$) presented in De Vito & Benvenuto (2010). For simplicity, we shall consider that β remains constant along each calculation. Then, we shall analyse the sensitivity of the evolutionary tracks due to changes in β . We shall be particularly interested in helium WDs, which are expected to be the type of objects found in some CBSs with accurate mass determinations (see below, Section 4).

The reminder of the paper is organized as follows. In Section 2, we present the main characteristics of our evolutionary code. In Section 3, we present and analyse the results obtained from our calculations. The main part of the paper ends in Section 4 where we discuss our results and make some concluding remarks. In Appendix A we present tables of our main numerical results, and the relation between WD mass and the final orbital period is given in Appendix B.

2 THE COMPUTER CODE

The code employed here has been presented in Benvenuto & De Vito (2003) where we described a generalized algorithm based on the Henyey technique that allows for the simultaneous computation of the donor stellar structure and the mass transfer rate in a fully implicit way. The code has updated physical ingredients. For temperatures $T > 6 \times 10^3 \text{ K}$, we considered radiative opacities given by Iglesias & Rogers (1996), while at lower temperatures we employed molecular opacities given by Ferguson et al. (2005). Conductive opacities have been taken from Itoh et al. (1983). Our equation of state has been that of Magni & Mazzitelli (1979). Nuclear reaction rates have been taken from Caughlan & Fowler (1988). Neutrino emission has been described following the works by Itoh & Kohyama (1983), Munakata, Kohyama & Itoh (1987) and Itoh et al. (1989, 1992). Diffusion processes (gravitational settling, chemical and thermal diffusion) have been accounted for following Althaus & Benvenuto (2000). We consider the mixing length theory as described in Kippenhahn, Weigert & Hofmeister (1967), setting the mixing length parameter l to $l/H_p = 1.7432$ (here H_p is the pressure scale height defined by $H_p \equiv dr/d\ln P$, where P denotes the total pressure and r is the distance measured from the stellar centre). Convective core overshoot is included as in Demarque et al. (2004). This important physical phenomenon consists in the presence of material motions and mixing beyond the canonical boundary for convection defined by the classic Schwarzschild criterion. A proper

treatment of convective core overshoot would require a radiative hydrodynamic treatment near the convective edge. The overshoot length is evaluated in terms of the local pressure scale height, multiplied by a constant parameter less than unity (Λ_{OS}). In their paper, Demarque et al. (2004) use values of Λ_{OS} from 0 to 0.2 depending on the value of the stellar mass compared to $M_{\text{crit}}^{\text{conv}}$ (the critical mass above which stars have a substantial convective core after pre-main-sequence phase). This value depends on the chemical composition. For further details, see Demarque et al. (2004). Furthermore, we considered grey atmospheres and neglected external irradiation due to the companion.

Let us now quote the physical ingredients we considered that are specifically related to binary evolution. To compute the radius R_L of a sphere with a volume equal to that of the Roche Lobe, we employed the standard expression given by Eggleton (1983). We adopted the mass transfer rate expression given by Ritter (1988). The orbital evolution has been computed following Rappaport, Joss & Webbink (1982) and Rappaport, Verbunt & Joss (1983). Mass and angular momentum losses have been described by two free parameters α and β (defined above). Gravitational radiation and magnetic braking were described as in Landau & Lifshitz (1975) and Verbunt & Zwaan (1981), respectively.

In our treatment of the orbital evolution, as stated above, we consider that the NS is able to retain a β fraction of the material coming from the donor star $\dot{M}_{\text{NS}} = \beta |\dot{M}|$ (where \dot{M} is the mass transfer rate from the donor star¹), as done in Benvenuto & De Vito (2005). We considered that β remains constant throughout all Roche lobe overflow (RLOF) episodes. Also, we assumed that material lost from the binary systems carries away the specific angular momentum of the compact object ($\alpha = 1$).

3 NUMERICAL RESULTS

We have constructed a grid of evolutionary models for the donor component of CBSs. We considered a wide range of initial masses M_i for the normal solar metallicity star ($M_i/M_{\odot} = 0.50, 0.65, 0.80, 1.00, 1.25, 1.50, 1.75, 2.00, 2.25, 2.50, 2.75, 3.00, 3.25$ and 3.50). For the mass $(M_{\text{NS}})_i$ of the accreting NS, we have selected four different initial values [$(M_{\text{NS}})_i/M_{\odot} = 0.80, 1.00, 1.20$ and 1.40].

While most of the known NS masses are around $1.4 M_{\odot}$, some NSs have masses clearly below that value. Good examples are the NSs in the X-ray binaries SMC X-1, Cen X-3 and 4U 1538–52 with masses of $1.17^{+0.16}_{-0.16}, 1.09^{+0.20}_{-0.36}$ and $0.96^{+0.19}_{-0.16} M_{\odot}$, respectively (Lattimer & Prakash 2004, 2007). This justifies our choice of $0.8 M_{\odot}$ as the minimum value for $(M_{\text{NS}})_i$. Very recently, Demorest et al. (2010) have detected a NS with a mass of $M_{\text{NS}} = 1.97 \pm 0.04 M_{\odot}$ in the PSR J1614–2230 binary system (with an orbital period of $8.686\,619\,4196$ d) orbiting together with a WD of $M = 0.500 \pm 0.006 M_{\odot}$. While this detection indicates that considering NSs with initial masses larger than $1.4 M_{\odot}$ should also be meaningful, note that the WD is too massive to have a helium-rich interior (see e.g. Iben & Tutukov 1985). Thus, this binary should not correspond to the class of systems we are interested in here.

We choose the initial orbital period of the systems P_i in order to obtain helium WDs or members of ultracompact binary systems (those in which the orbital period is less than 1 h; see e.g. Fedorova & Ergma 1989; van der Sluys, Verbunt & Pols 2005) as the final state of the donor stars. Besides, for each group of initial parameters

(masses of the components and orbital periods), we have considered five values of β (0.00, 0.25, 0.50, 0.75 and 1.00) for the cases of $(M_{\text{NS}})_i/M_{\odot} = 0.80, 1.00$ and 1.20 , and refined our grid considering a step of $\Delta\beta = 0.125$ for the case of $(M_{\text{NS}})_i = 1.40 M_{\odot}$. We have performed more than a thousand evolutionary sequences in which we have followed the evolution of the donor star from the zero-age main sequence (ZAMS) on. In order to end our calculations, we have considered several situations. As we are interested in helium WDs, we only consider objects with a central temperature $\log_{10}(T_c/K) < 8$, below the threshold for helium burning. Also, we stop if the mass transfer rate exceeds a value of $10^{-5} M_{\odot} \text{ yr}^{-1}$, or if the mass of the accreting NS is greater than $2.5 M_{\odot}$. This value is larger than the maximum mass of NS corresponding to many nuclear matter equations of state (Lattimer & Prakash 2004). In the case of systems that evolve to an open configuration, we stopped computations if the WD luminosity is $\log_{10}(L/L_{\odot}) \leq -5$ or if it is much older (20 Gyr) than the Universe. In the case of ultracompact systems, we ended the calculations when $M \leq 0.050 M_{\odot}$ or $P \leq 0.05$ d.

As we varied the parameters defining the CBS over a wide range of values, it is not surprising that we have found a large variety of evolutionary paths. In some cases, the mass transfer episode is stable and the rate of mass exchange is self-regulated, while in others $|\dot{M}|$ increases to extreme values, leading to common envelope evolution.

It is known that a dynamical mass transfer instability occurs when the radius of the Roche lobe shrinks more rapidly (or expands less slowly) than the donor star. The adiabatic response of a star to mass loss has long been understood (see e.g. Hjellming & Webbink 1987). Stars with radiative envelopes (e.g. upper main-sequence stars) contract in response to mass loss, while stars with convective envelope (e.g. lower main-sequence or red giant stars) expand (for a detailed explanation, see e.g. Soberman, Phinney & van den Heuvel 1997; Podsiadlowski et al. 2002). When the donor star is perturbed by removal of some mass, it falls out of hydrostatic and thermal equilibrium. In the process of re-establishing equilibrium, the star will either grow or shrink. Also, the Roche lobe changes in response to the mass transfer/loss. As long as the donor star's Roche lobe continues to enclose the star, mass transfer is stable. Otherwise, it is unstable and proceeds on a dynamical time-scale. We define for the donor star and its Roche lobe $\zeta_{\text{donor}} = \partial \ln R / \partial \ln M$ and $\zeta_L = \partial \ln R_L / \partial \ln M$, respectively. The stability of mass transfer is determined by a comparison of ζ_{donor} and ζ_L . Given $R \cong R_L$ (the condition for the onset of RLOF), the initial stability criterion is $\zeta_L \leq \zeta_{\text{donor}}$. Tauris & Savonije (1999) have studied the behaviour of $\zeta_L(q, \beta)$ for LMXBs, where $q = M/M_{\text{NS}}$. They found that ζ_L does not depend strongly on β , which is in agreement with our calculations (see Tables A1–A4). These authors found that, in general, the Roche lobe increases ($\zeta_L < 0$) when material is transferred from a light donor to a heavier NS ($q < 1$) and correspondingly R_L decreases ($\zeta_L > 0$) when material is transferred from a heavier donor to a lighter NS ($q > 1$). These are the cases (a large value of q and/or stars with convective envelope) where we find unstable mass transfer situations.

On the contrary, for the case of the most massive initial NSs, our grid extends to initial masses of the donor star up to $3.5 M_{\odot}$. In this case, the calculations are stopped because of the onset of helium burning at the stellar core [$\log_{10}(T_c/K) \geq 8$] or because the NS mass exceeds the upper limit we have chosen (especially in the case of $\beta = 1$). If we consider higher initial values for the mass of the NS, this situation would be found more frequently. Presumably, these CBSs should lead to BH formation. Another interesting result is that the range of initial periods for which CBSs lead to the formation

¹ We use absolute value because, according to our definition, \dot{M} is a negative quantity.

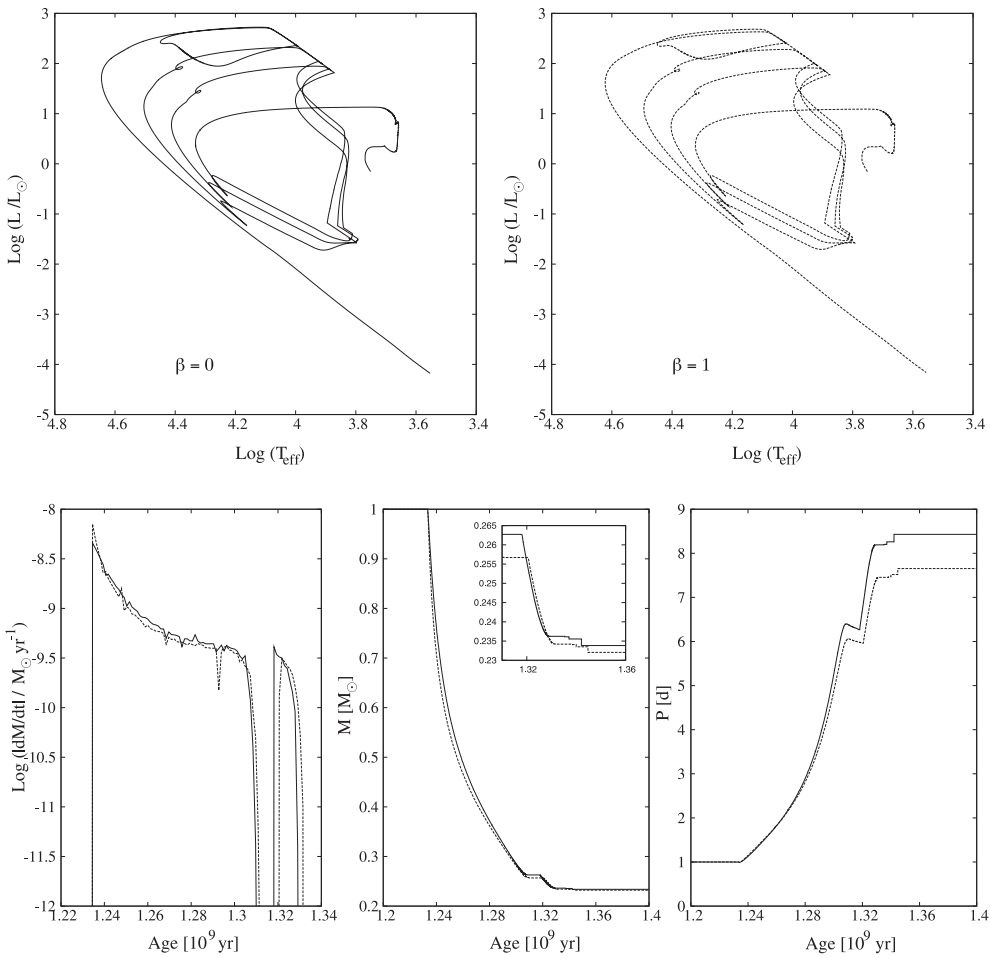


Figure 1. Upper panels show the evolutionary tracks of the donor component of a CBS with initial mass $M_i = 1 M_{\odot}$ for the donor star, $(M_{NS})_i = 1.40 M_{\odot}$ for the NS, and an initial orbital period of $P_i = 1.5$ d. The three loops in the HR diagrams are due to hydrogen shell flashes, and very little mass transfer is associated with any beyond the first mass transfer episode (for details, see main text). The left-hand (right-hand) panel corresponds to the case of $\beta = 0.0$ (1.0). Lower panels show the results corresponding to the same evolutionary calculations related to the evolution of the mass transfer rate during the first RLOF (left-hand panel), donor mass (middle panel) and orbital period (right-hand panel). Note that the final period is slightly dependent on β , while the others are almost unaffected.

of converging systems extends to higher initial orbital periods (P_i) with decreasing values of $(M_{NS})_i$.

In order to analyse the changes in the evolution of open CBSs by varying β , we may choose the set of models corresponding to donor stars with initial mass $M_i = 1.00 M_{\odot}$, a NS with initial mass $(M_{NS})_i = 1.40 M_{\odot}$, initial orbital period of $P_i = 1.5$ d and extreme values of β (0 and 1) as a representative case. On the upper panels of Fig. 1 we present the evolutionary tracks of the donor star for these systems.

After core hydrogen exhaustion, the donor star evolves towards the red giant region of the Hertzsprung–Russell (HR) diagram, overflowing its corresponding Roche lobe. Since then, the star undergoes the first RLOF mass transfer episode. After losing approximately 70 per cent of its initial mass, the outer hydrogen envelope embraces a so little mass fraction that it is no longer able to stand as a giant and starts a fast contraction to become a pre-WD star. This contraction heats up the bottom of the hydrogen envelope that now is partially degenerate; meanwhile, diffusion has led some hydrogen inwards. Then a thermonuclear hydrogen flash starts, leading to a sudden swell of the outer layers that overflow the Roche lobe again. Now the amount of transferred matter is far lower (approximately

$10^{-3} M_{\odot}$) than that lost by the donor star during the first RLOF. This transferred mass, together with the nuclear burning, still active at the bottom of the hydrogen envelope, contribute to lower the total hydrogen content of the star. This forces the star to undergo a new contraction to become a pre-WD star again. In this set of models, the donor star undergoes three flashes before evolving to the final WD cooling track. A more detailed discussion of the evolution of this kind of systems has been presented in Benvenuto & De Vito (2004).

Note that the evolutionary tracks shown in Fig. 1 are barely dependent on β . The same is found when we analyse the evolution of the mass transfer rate and the mass of the donor star, as shown in the bottom-left and middle panels of Fig. 1. More significant changes are found for the evolution of the orbital period, as shown in the bottom-right panel of Fig. 1.

From the analysis given above, we find that changes in β induce smooth changes in the configuration of the resulting CBSs. In view of this fact, we have constructed surfaces to study the behaviour of the masses of both stars and the final orbital period as functions of β and $\log_{10}(P_i/d)$. As we are interested in the formation of helium WDs, the surfaces cover an ample region of the parameter space only

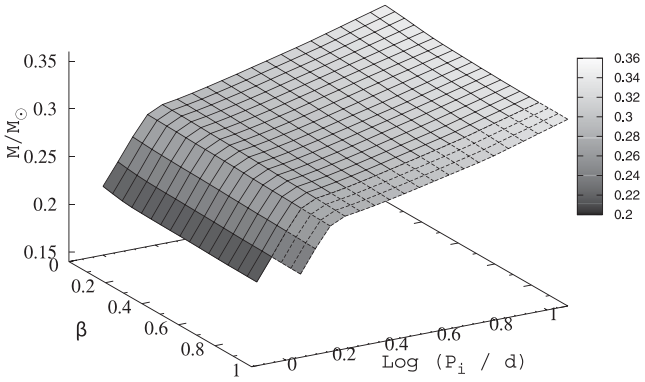
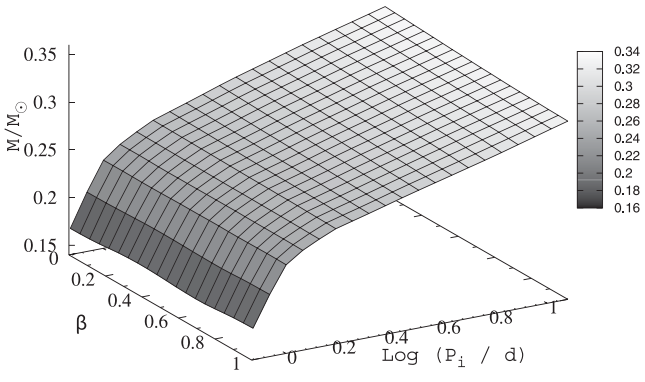
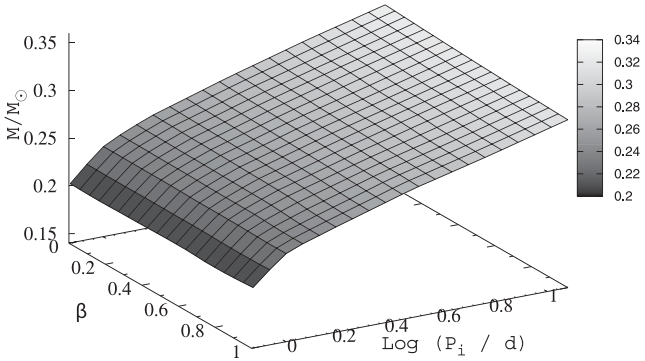


Figure 2. The final mass of the donor star for the case of systems with $(M_{\text{NS}})_i = 1.4 M_{\odot}$ and normal stars with $M_i = 1.00 M_{\odot}$ (upper panel), $M_i = 1.25 M_{\odot}$ (middle panel) and $M_i = 1.50 M_{\odot}$ (bottom panel) as a function of the logarithm of the initial orbital period P_i (in days) and the fraction β of the mass that can be accreted by the NS. The surface corresponding to the case of an initial donor mass of $1.50 M_{\odot}$ does not extend on a rectangular region because in the region not shown, the mass of the NS gets larger than $2.50 M_{\odot}$. Note that the grey-scale on the surface indicates the mass values.

for the case of donors with low initial masses (say $1.00\text{--}1.50 M_{\odot}$); for higher initial donor masses, surfaces are much narrower. These surfaces give a direct insight into the dependence of evolutionary sequences on the parameter β . In Fig. 2, we show the mass of the donor star remnant as a function of β and $\log_{10}(P_i/d)$ for systems with initial masses M_i/M_{\odot} of 1.00, 1.25 and 1.50 for the donor star and $(M_{\text{NS}})_i = 1.40 M_{\odot}$ for the NS component. In Fig. 3, we

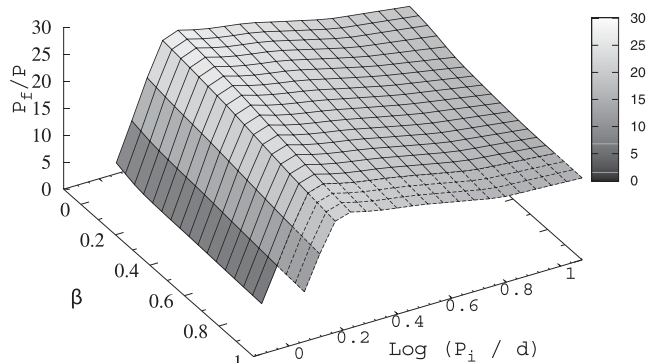
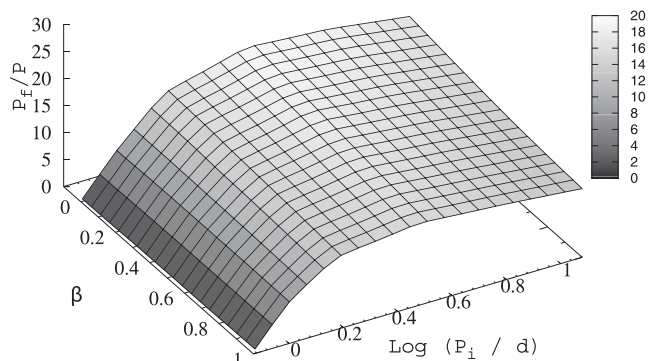
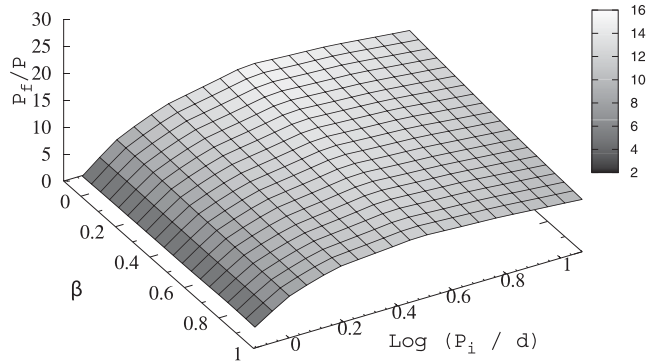


Figure 3. The ratio of the final to the initial orbital period for the case of systems with $(M_{\text{NS}})_i = 1.4 M_{\odot}$ and normal stars with $M_i = 1.00 M_{\odot}$ (upper panel), $M_i = 1.25 M_{\odot}$ (middle panel) and $M_i = 1.50 M_{\odot}$ (bottom panel) as a function of the logarithm of the initial orbital period P_i (in days) and the fraction β of the mass that can be accreted by the NS. The surface corresponding to the case of an initial donor mass of $1.50 M_{\odot}$ does not extend on a rectangular region because in the region not shown, the mass of the NS gets larger than $2.50 M_{\odot}$. As in Fig. 2, the grey-scale on the surface corresponds to the value of the function on the vertical axis.

show the ratio of the final to the initial orbital periods for the same models included in Fig. 2.

In order to present our results regarding the final NS mass, we found it useful to make a simple transformation. In our models, we have assumed that

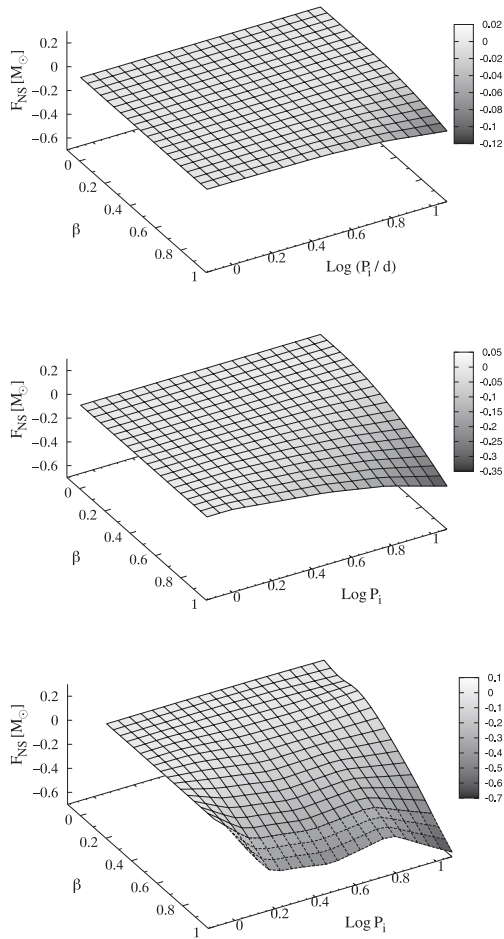


Figure 4. The function $F_{\text{NS}} = M_{\text{NS}} - (M_{\text{NS}})_i + \beta(M - M_i)$ (defined in equation 3) for the case of systems with $(M_{\text{NS}})_i = 1.4 M_{\odot}$ and normal stars with $M_i = 1.00 M_{\odot}$ (upper panel), $M_i = 1.25 M_{\odot}$ (middle panel) and $M_i = 1.50 M_{\odot}$ (bottom panel) as a function of the logarithm of the initial orbital period P_i (in days) and the fraction β of the mass that can be accreted by the NS. The surface corresponding to the case of an initial donor mass of $1.50 M_{\odot}$ does not extend on a rectangular region because in the region not shown, the mass of the NS gets larger than $2.50 M_{\odot}$. F_{NS} gives the amount of material lost from the binary system because of super-Eddington accretion rates on to the NS. If $M_{\text{NS}} \leq \dot{M}_{\text{Edd}}$ were fulfilled during all RLOFs, then $F_{\text{NS}} = 0$. The departure of F_{NS} from zero is barely noticeable for the case of a donor star of $M_i = 1.00 M_{\odot}$. However, for the case of $M_i/M_{\odot} = 1.25$ and 1.50, the surfaces get larger negative values the larger β and P_i . These conditions correspond to short RLOF episodes when the donor is a red giant undergoing super-Eddington transfer rates. As in Fig. 2, the grey-scale on the surface corresponds to the value of the function on the vertical axis.

$$\dot{M}_{\text{NS}} = \text{Min}(\beta|\dot{M}|, \dot{M}_{\text{Edd}}). \quad (1)$$

If $\beta|\dot{M}| \leq \dot{M}_{\text{Edd}}$ were fulfilled throughout the entire evolution of the system, we may integrate it, finding that

$$M_{\text{NS}} - (M_{\text{NS}})_i = -\beta(M - M_i), \quad (2)$$

where M and M_{NS} stand for the final WD and NS masses, respectively. Therefore, we may define F_{NS} as

$$F_{\text{NS}} = M_{\text{NS}} - (M_{\text{NS}})_i + \beta(M - M_i). \quad (3)$$

Clearly, if $\dot{M}_{\text{NS}} \leq \dot{M}_{\text{Edd}}$ is fulfilled in all RLOFs, then $F_{\text{NS}} = 0$. Thus, F_{NS} (equation 3) shows the effects due to the stages at which $\dot{M}_{\text{NS}} > \dot{M}_{\text{Edd}}$ forcing a supplementary mass-loss rate from the system apart from the $(1 - \beta)|\dot{M}|$ contribution. In Fig. 4, we show the surface defined by F_{NS} for the same set of models included in Figs 2–3.

In view of the fact that the surfaces shown in Figs 2–4 are very smooth, it is useful to represent them by a suitable function $F(x, y)$. We found it adequate to consider the quotient of polynomials given by

$$F(x, y) = \frac{C_1 + C_2x + C_3y + C_4x^2 + C_5y^2 + C_6xy}{1 + C_7x + C_8y}, \quad (4)$$

where we assign $x = \beta$ and $y = \log_{10}(P_i/d)$. The coefficients $C_i, i = 1, \dots, 8$, are found by standard least-squares method, and the results are given in Table 1. These fits allow for an immediate calculation of the final orbital period and donor mass values. To compute the final NS mass, we have first to compute donor star mass and then apply equation (3).

These fits provide a useful description of the dependence of the characteristics of these systems on β and $\log_{10}(P_i/d)$. While these surfaces correspond to the cases of initial masses of $M_i/M_{\odot} = 1.00, 1.25$ and 1.50 and $(M_{\text{NS}})_i = 1.40 M_{\odot}$, it should be stressed that in defining the surfaces we do not have to compute a large number of time-consuming binary evolutionary sequences. If necessary, this technique may be extended to other values of donor and NS masses employing the results given in Tables A1–A4.

As stated above, for the case of more massive donor stars, the range of initial periods for which CBSs evolve to produce helium WDs is much narrower, making it impossible to construct surfaces similar to those already presented. In Fig. 5, we show 2D plots for selected systems, showing the dependence of the final masses and period of these systems on β . The behaviour of these quantities is similar to that found for the case of less massive donor stars.

4 DISCUSSION AND CONCLUSIONS

In this paper, we have computed the evolution of CBSs composed of a normal solar composition, donor star and a NS companion. The range of masses and periods has been chosen in order to study CBSs that evolve to open, helium WD–MSP pairs or to ultracompact systems. In order to compute the orbital evolution of these systems, we have considered that the NS is able to accrete a β fraction of the mass coming from the donor star. We assumed an upper limit for the accretion rate of the NS imposed by the Eddington accretion rate (see Section 1). In previous works, we have studied the evolution of CBSs varying the initial configuration, defined by the orbital period, and the masses of the donor and NS. In this work, we explored the evolution of CBSs for a variety of values of β .

While our model results are given in Tables A1–A4, in some favourable cases we have been able to construct surfaces for the final mass of the donor star, the orbital period and the mass of the NS by means of the function F_{NS} given in equation (3). Also, we presented fits (equation 4 and Table 1) to these surfaces that allow for a fast evaluation of the final CBS configuration as a function of P_i and β . It is clear that, in the case of the systems that evolve to an open configuration, the mass of the resulting WD is barely sensitive to the value of β . The final orbital period, in most cases (for a given initial configuration), exhibits moderate changes of approximately 25 per cent. However, in some particular cases, changes are even larger

Table 1. Values of the coefficients corresponding to the fit of the function defined in equation (4) to the surfaces shown in Figs 2–4. In the last column, we give the maximum relative error of the fit with respect to the numerical results. In most regions of these surfaces, the error is much smaller.

M/M_{\odot}	Fit to $M_f(M_{\odot})$								Error
	C_1	C_2	C_3	$1000 \times C_4$	C_5	C_6	C_7	C_8	
1.00	0.233 00	-0.034 933	1.029 46	-0.678 79	0.240 747	-0.057 173	-0.1430 95	3.701 49	5 per cent
1.25	0.228 53	-0.027 247	1.203 25	-0.514 58	0.244 226	-0.064 110	-0.1253 05	4.087 25	1 per cent
1.50	0.208 05	-0.031 279	2.916 13	7.296 67	0.463 526	-0.109 318	-0.090 219	9.693 35	1 per cent
M/M_{\odot}	Fit to P_f/P_i								Error
	C_1	C_2	C_3	C_4	C_5	C_6	C_7	C_8	
1.00	8.482 58	0.115 165	41.7855	0.502 319	-18.7955	-6.800 65	0.212 949	1.367 73	5 per cent
1.25	8.424 98	-0.317 404	65.9782	0.129 753	-30.7561	-10.5503	0.076 967	1.5722	1 per cent
1.50	4.212 98	-2.180 37	387.409	1.420 05	-180.716	-50.0681	0.299 583	10.352	2 per cent
M/M_{\odot}	Fit to $F_{NS}(M_{\odot})$								Error
	$100 \times C_1$	$100 \times C_2$	$100 \times C_3$	$100 \times C_4$	$100 \times C_5$	C_6	C_7	C_8	
1.00	-0.450 35	1.630 95	1.214 02	-1.353 00	-0.642 33	-0.017 375	-0.454 202	-0.390 476	10 per cent
1.25	-1.167 27	6.381 60	3.613 86	-6.211 25	-1.625 58	-0.105 957	-0.351 645	-0.332 994	3 per cent
1.50	-1.194 52	3.220 75	14.5978	-2.165 77	-4.700 89	-0.730 932	-0.901 429	1.134 020	5 per cent

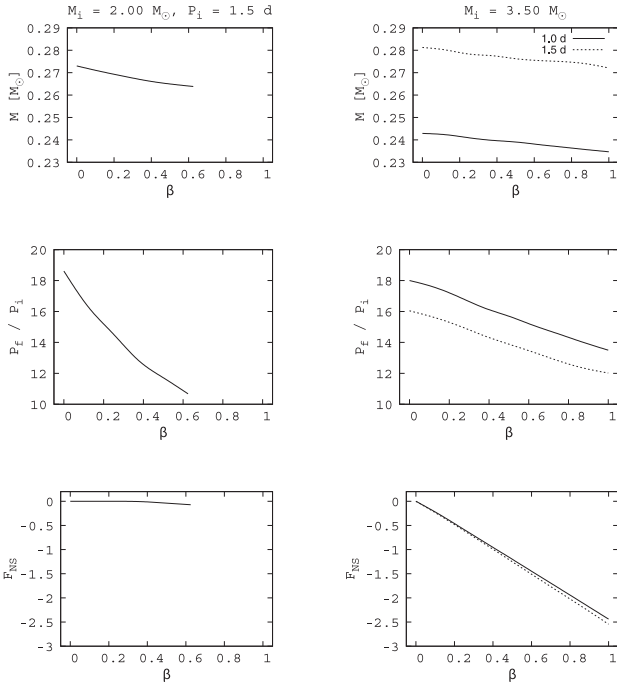


Figure 5. The final mass of the donor star (upper panels), the ratio of the final to the initial orbital period (middle panels) and the function $F_{NS} = M_{NS} - (M_{NS})_i + \beta(M - M_i)$ [defined in equation (3), see also Fig. 4] (lower panels) as a function of β . Left-hand panels correspond to systems with $(M_{NS})_i = 1.4 M_{\odot}$ and $M_i = 2.00 M_{\odot}$, $P_i = 1.5$ d, while right-hand panels depict the cases of the same initial NS mass and $M_i = 3.50 M_{\odot}$, $P_i = 1.0$ d and 1.5 d. For these high-mass values of the donor star, the range of initial periods that produce a helium WD is much more restricted, which does not allow for constructing surfaces like those presented in Figs 2–4.

than 100 per cent (see e.g. in Table A2 the case of $M_i = 2.50 M_{\odot}$, $(M_{NS})_i = 1.00 M_{\odot}$, $P_i = 1.50$ d). As expected, the most sensitive quantity is the final NS mass.

The grid presented in this paper should be useful to study the characteristics of CBSs composed of low-mass WDs and MSPs. There are five systems of this kind (see Table 2) in which the masses of the components have been measured with high precision thanks to the detection of the relativistic Shapiro delay in pulsar

timing (see Taylor & Weisberg 1989, and references therein). Let us now discuss the possibility of inferring the value of β from the available data of these systems.

Looking for a progenitor configuration of a CBS is a way to test the theory of CBS evolution. If correct, we should be able to find plausible initial configurations. The most sensitive quantity to changes of β is the final NS mass. In order to recycle a NS, we do need a minimum amount of mass to be accreted (see Cook, Shapiro & Teukolsky 1994). The exact value of such minimum amount of mass depends on the initial rotation rate of the NS and on the still uncertain cold nuclear matter equation of state. This uncertainty, together with the unknown initial mass and spin of the NS, prevents us from employing the observational data available on the NS to further constrain the parameter space for the initial configuration. Remarkably, WD properties are barely dependent on β , while in most cases the orbital period shows a moderate dependence on this parameter. Thus, it is very difficult to determine β by means of evolutionary studies. This would be the case even if the masses of the components of the systems were known far more accurately.

In this work, as usual, we considered the value of β as constant. Of course, this may not be the actual case. If so, our β could be considered as a kind of effective mean value. In any case, our results indicate that if we are interested in the evolution of the donor star moving on a circular orbit, considering a fixed β is justified. Including modelling of physical processes that may modulate the accretion rate on to the NS (e.g. magnetic field evolution) has a minor effect on the results presented in this paper. Thus, these improvements are not warranted in this context.

Another interesting issue is the fact that existing models do not reproduce the orbital period distribution of binary MSP well. Also, the proposition that LMXBs are progenitors of binary MSPs has the difficulty that the birth rates of both types of systems do not match each other. Very recently, Hurley et al. (2010) performed an exhaustive study of the birth rate of LMXBs and binary MSPs and their orbital period distributions. These authors considered the formation of NSs that become MSPs as due to core-collapse supernovae and accretion-induced collapse of oxygen/neon WDs. Figs 4–6 of Hurley et al. (2010) show the theoretical and observed orbital period distribution of binary MSPs. Despite the amount of details considered in that study, they found a poor agreement. In this paper, we have found some dependence of the final orbital period on the value

Table 2. The CBSs composed of a MSP and a low-mass WD for which it has been possible to detect the Shapiro delay effect and measure the masses of both components. All these systems belong to the Galactic plane population. From left to right, the table presents the name of the pulsar, its spin period, the WD and pulsar masses, the orbital period and the relevant reference, respectively.

Name	P_p (ms)	M_{WD} (M_\odot)	M_{NS} (M_\odot)	P (d)	Reference
PSR J0437-4715	5.757	0.236 ± 0.017	1.58 ± 0.18	5.741	van Straten et al. (2001)
PSR J1614+2230	3.15	0.500 ± 0.006	1.97 ± 0.04	8.687	Demorest et al. (2010)
PSR J1713+0747	4.57	0.28 ± 0.03	1.3 ± 0.2	67.825	Splaver et al. (2005)
PSR B1855+09	5.362	$0.258^{+0.028}_{-0.016}$	$1.50^{+0.26}_{-0.14}$	12.327	Kaspi, Taylor & Ryba (1994)
PSR J1909-3744	2.947	0.2038 ± 0.0022	1.438 ± 0.024	1.533	Jacoby et al. (2005)

of β . Considering this effect in the context of the orbital period distribution of binary MSPs may help us to bring theoretical predictions closer to observations. This possibility certainly deserves a detailed study.

ACKNOWLEDGMENT

The authors would like to thank the anonymous referee for his/her very useful and constructive reports that guided them to largely improve the original version of this paper.

REFERENCES

- Althaus L. G., Benvenuto O. G., 2000, MNRAS, 317, 952
 Benvenuto O. G., De Vito M. A., 2003, MNRAS, 342, 50
 Benvenuto O. G., De Vito M. A., 2004, MNRAS, 352, 249
 Benvenuto O. G., De Vito M. A., 2005, MNRAS, 362, 891
 Benvenuto O. G., Rohrman R. D., De Vito M. A., 2006, MNRAS, 366, 1520
 Bhattacharya D., van den Heuvel E. P. J., 1991, Phys. Rep., 203, 1
 Caughlan G. R., Fowler W. A., 1988, Atomic Data Nuclear Data Tables, 40, 283
 Church M. J., Inogamov N. A., Balucińska-Church M., 2002, A&A, 390, 139
 Cook G. B., Shapiro S. L., Teukolsky S. A., 1994, ApJ, 423, L117
 De Vito M. A., Benvenuto O. G., 2010, MNRAS, 401, 2552
 Demarque P., Woo J.-H., Kim Y.-C., Yi S. K., 2004, ApJS, 155, 667
 Demorest P. B., Pennucci T., Ransom S. M., Roberts M. S. E., Hessels J. W. T., 2010, Nat, 467, 1081
 Eggleton P. P., 1983, ApJ, 268, 368
 Ergma E., Sarna M. J., Antipova J., 1998, MNRAS, 300, 352
 Fedorova A. V., Ergma E. V., 1989, AP&SS, 151, 125
 Ferguson J. W., Alexander D. R., Allard F., Barman T., Bodnarik J. G., Hauschildt P. H., Heffner-Wong A., Tamanai A., 2005, ApJ, 623, 585
 Hjellming M. S., Webbink R. F., 1987, ApJ, 318, 794
 Hurley J. R., Tout C. A., Wickramasinghe D. T., Ferrario L., Kiel P. D., 2010, MNRAS, 402, 1437
 Iben I., Jr, Tutukov A. V., 1985, ApJS, 58, 661
 Iglesias C. A., Rogers F. J., 1996, ApJ, 464, 943
 Itoh N., Kohyama Y., 1983, ApJ, 275, 858
 Itoh N., Mitake S., Iyetomi H., Ichimaru S., 1983, ApJ, 273, 774
 Itoh N., Adachi T., Nakagawa M., Kohyama Y., Munakata H., 1989, ApJ, 339, 354
 Itoh N., Mutoh H., Hikita A., Kohyama Y., 1992, ApJ, 395, 622
 Jacoby B. A., Hotan A., Bailes M., Ord S., Kulkarni S. R., 2005, ApJ, 629, L113
 Joss P. C., Rappaport S., Lewis W., 1987, ApJ, 319, 180
 Kaspi V. M., Taylor J. H., Ryba M. F., 1994, ApJ, 428, 713
 Kippenhahn R., Weigert A., Hofmeister E., 1967, Methods Comput. Phys., 7, 129.
 Kulkarni A. K., Romanova M. M., 2009, MNRAS, 398, 701
 Landau L. D., Lifshitz E. M., 1975, The Classical Theory of Fields. Pergamon Press, Oxford
 Lattimer J. M., Prakash M., 2004, Sci, 304, 536
 Lattimer J. M., Prakash M., 2007, Phys. Rep., 442, 109
 Magni G., Mazzitelli I., 1979, A&A, 72, 134
 Mitsuda K., Inoue H., Nakamura N., Tanaka Y., 1989, PASJ, 41, 97
 Munakata H., Kohyama Y., Itoh N., 1987, ApJ, 316, 708
 Nelson L. A., Rappaport S., 2003, ApJ, 598, 431
 Nelson L. A., Dubeau E., MacCannell K. A., 2004, ApJ, 616, 1124
 Podsiadlowski P., Joss P. C., Hsu J. J. L., 1992, ApJ, 391, 246
 Podsiadlowski P., Rappaport S., Pfahl E. D., 2002, ApJ, 565, 1107
 Rappaport S., Joss P. C., Webbink R. F., 1982, ApJ, 254, 616
 Rappaport S., Verbunt F., Joss P. C., 1983, ApJ, 275, 713
 Rappaport S., Podsiadlowski P., Joss P. C., Di Stefano R., Han Z., 1995, MNRAS, 273, 731
 Ritter H., 1988, A&A, 202, 93
 Romanova M. M., Kulkarni A. K., Long M., Lovelace R. V. E., 2008, in Wijnands R., Altamirano D., Soleri P., Degenaar N., Rea N., Casella P., Pastrun A., Linares M., eds, AIP Conf. Proc. Vol. 1068, A Decade of Accreting Millisecond X-ray Pulsars. Am. Inst. Phys., New York, p. 87
 Shakura N. I., Sunyaev R. A., 1973, A&A, 24, 337
 Shakura N. I., Sunyaev R. A., 1976, MNRAS, 175, 613
 Soberman G. E., Phinney E. S., van den Heuvel E. P. J., 1997, A&A, 327, 620
 Splaver E. M., Nice D. J., Stairs I. H., Lommen A. N., Backer D. C., 2005, ApJ, 620, 405
 Takahashi H., Makishima K., 2006, in Wilson A., ed., in ESA SP-604, The X-ray Universe 2005. ESA Publications, Noordwijk, p. 309
 Tauris T. M., Savonije G. J., 1999, A&A, 350, 928
 Taylor J. H., Weisberg J. M., 1989, ApJ, 345, 434
 van der Sluys M. V., Verbunt F., Pols O. R., 2005, A&A, 431, 647
 van Straten W., Bailes M., Britton M., Kulkarni S. R., Anderson S. B., Manchester R. N., Sarkissian J., 2001, Nat, 412, 158
 Verbunt F., Zwaan C., 1981, A&A, 100, L7
 White N. E., Stella L., Parmar A. N., 1988, ApJ, 324, 363

APPENDIX A: THE GRID OF MODELS

In Tables A1–A4, we present the main results of our calculations. Each table corresponds to a fixed value of the initial mass of the NS ($M_{\text{NS}})_i$ and gives the final masses of the donor and NS (M and M_{NS} , respectively), and the final orbital period P_f for each initial configuration (defined by the initial mass of the donor star M_i , the initial orbital period P_i and β). We do not present results corresponding to initial donor masses of 0.50, 0.65 and $0.80 M_\odot$ because the corresponding systems produce donor star with final masses of $0.05 M_\odot$ or eventually the donor star overfill its Roche lobe on the ZAMS.

Table A3 – continued

β	P_{f} (d)	M (M_{\odot})	M_{NS} (M_{\odot})	P_{f} (d)	M (M_{\odot})	M_{NS} (M_{\odot})	P_{f} (d)	M (M_{\odot})	M_{NS} (M_{\odot})	P_{f} (d)	M (M_{\odot})	M_{NS} (M_{\odot})	P_{f} (d)	M (M_{\odot})	M_{NS} (M_{\odot})	P_{f} (d)	M (M_{\odot})	M_{NS} (M_{\odot})	P_{f} (d)	M (M_{\odot})	M_{NS} (M_{\odot})					
		$P_{\text{i}} = 0.50 \text{ d}$			$P_{\text{i}} = 0.75 \text{ d}$				$P_{\text{i}} = 1.00 \text{ d}$				$P_{\text{i}} = 1.50 \text{ d}$			$P_{\text{i}} = 2.50 \text{ M}_{\odot}$		$P_{\text{i}} = 3.00 \text{ d}$			$P_{\text{i}} = 6.00 \text{ d}$			$P_{\text{i}} = 12.00 \text{ d}$		
0.00	0.048	0.050	1.200	0.040	0.050	1.200	0.042	0.049	1.200	2.490	0.211	1.200					$\log T_c \geq 8$									
0.25	0.048	0.050	1.596	0.041	0.050	1.571	0.043	0.050	1.555	3.456	0.221	1.495					$\log T_c \geq 8$									
0.50	0.050	0.050	1.922	0.042	0.049	1.874	0.043	0.049	1.851	3.676	0.222	1.736					$\log T_c \geq 8$									
0.75	0.049	0.050	2.228	0.042	0.050	2.168	0.044	0.050	2.123	3.737	0.223	1.961					$\log T_c \geq 8$									
1.00		$M_{\text{NS}} \geq 2.5$		0.042	0.050	2.460	0.044	0.050	2.401	3.708	0.223	2.181					$\log T_c \geq 8$									
0.00			\dot{M} in ZAMS		0.040	0.050	1.200	0.042	0.049	1.200	6.720	0.239	1.200													
0.25	0.050	0.050	1.545	0.041	0.049	1.538	0.042	0.049	1.519	7.465	0.243	1.439														
0.50	0.051	0.050	1.810	0.041	0.049	1.804	0.043	0.049	1.777	7.224	0.240	1.621														
0.75	0.050	0.050	2.086	0.042	0.050	2.093	0.043	0.049	2.037	6.629	0.239	1.809														
1.00	0.050	0.050	2.343	0.042	0.050	2.363	0.044	0.050	2.289	6.446	0.238	1.988														
0.00			\dot{M} in ZAMS		0.041	0.050	1.200	0.049	0.050	1.200	14.798	0.262	1.200													
0.25			\dot{M} in ZAMS		0.041	0.050	1.481	0.033	0.050	1.467	13.888	0.261	1.386													
0.50			\dot{M} in ZAMS		0.041	0.050	1.711	0.043	0.050	1.702	12.748	0.258	1.539													
0.75			\dot{M} divergent		0.041	0.050	1.934	0.050	0.050	1.934	11.713	0.256	1.686													
1.00			\dot{M} divergent		0.042	0.050	2.157	0.018	0.050	2.142	11.579	0.256	1.825													
0.00			\dot{M} divergent				\dot{M} divergent	9.088	0.224	1.200	13.606	0.269	1.200													
0.25			\dot{M} divergent				\dot{M} divergent	8.662	0.223	1.399	14.804	0.246	1.390													
0.50			\dot{M} in ZAMS				\dot{M} divergent			12.625	0.257	1.498														
0.75			\dot{M} divergent				\dot{M} divergent			11.5265	0.257	1.633														
1.00			\dot{M} divergent				\dot{M} divergent	6.767	0.217	1.920	11.679	0.240	1.927													

APPENDIX B: THE RELATION BETWEEN THE MASS OF THE WHITE DWARF AND THE FINAL ORBITAL PERIOD

The mass of WDs resulting from the evolution of CBSs satisfies a relation with the final orbital period of the system. This relation has been studied previously by e.g. Rappaport et al. (1995), Tauris & Savonije (1999) and Nelson, Dubeau & MacCannell (2004). Recently, we have examined quantitatively the predictions made by the authors previously mentioned, and proposed a new relation from our own calculations (De Vito & Benvenuto 2010). In that work, we considered the evolution of donor stars of CBSs with different masses of the accreting NSs but a fixed value of β ($= 0.5$). Now, we add to these calculations the results corresponding to different values of the parameter β . This is shown in Fig. B1, where we show the results corresponding to open systems and to converging systems in which the mass of the donor star is larger than $0.15 M_{\odot}$ (in these cases, we plot the value of the orbital period at an age of 13 Gyr). We observe from Fig. B1 that the dispersion in the relation we have plotted decreases as we move towards larger masses of the WD and orbital periods. This is because, in these cases, the donor star is on the red giant branch at the beginning of the first mass transfer episode, and then the core mass–radius relation is well satisfied (Joss, Rappaport & Lewis 1987).

The WD mass–orbital period relation presented in Fig. B1 is based on five times more models than that shown in De Vito & Benvenuto (2010), which makes the relation shown here a more solid result. In any case, we should remark that the analytical fitting found in our previous paper is in nice agreement with these new results. A variation of the value of β produces a motion of the point at most in the size of the symbols employed in the figure.

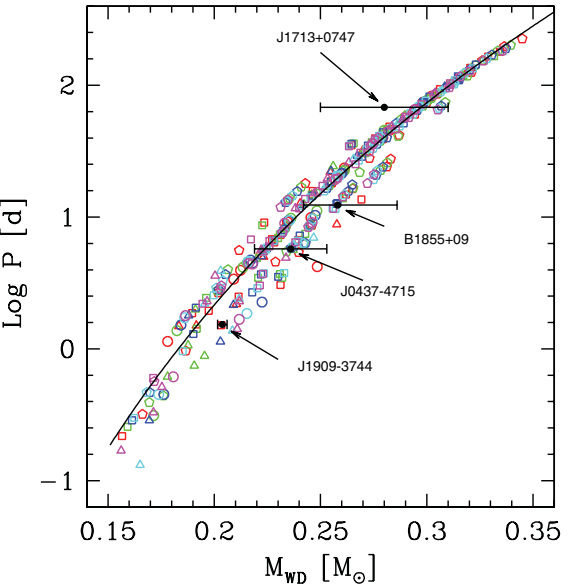


Figure B1. The relation between the mass of the WD and the final orbital period. We present with circles, triangles, squares and pentagons the cases of accreting NSs with initial mass values of $0.80, 1.00, 1.20$ and $1.40 M_{\odot}$, respectively. The colours red, green, blue, sky blue and magenta correspond to the cases of $\beta = 0.00, 0.25, 0.50, 0.75$ and 1.00 , respectively. Solid line represents the fit to the $M_{\text{WD}}-P$ relation $P = 2.6303 \times 10^6 (M_{\text{WD}}/M_{\odot})^{8.7078} \text{ d}$ given in De Vito & Benvenuto (2010). We have plotted, in addition, data corresponding to four helium WDs belonging to CBSs, companions of MSPs, whose masses are known.

This paper has been typeset from a $\text{\TeX}/\text{\LaTeX}$ file prepared by the author.